

# Validity of Cross-Spectrum PN Measurement

Ajay K. Poddar  
Synergy Microwave, USA

Ulrich L. Rohde  
BTU Cottbus, Germany

Enrico Rubiola  
FEMTO-ST Institute, France

Karl-Heinz Hoffmann  
Bayerische Akademie, Germany

**Abstract**—This paper reports the anomaly of instruments that uses cross-spectrum method for the measurement of oscillator phase noise. Although, cross-spectrum techniques facilitate high sensitivity by correlation and averaging, it can give disingenuous measurement data depending upon many unknowns (phase-inversion, multi-mode spectrum associated with negative index dynamics, odd order harmonics, impedance/phase mismatch, and thermal energy) that are not taken into account. Most of the time errors in PN (phase noise) measurement is within the limit but this is not true for ultra low phase noise crystal oscillator and oscillator that uses negative index ( $\epsilon < 0$ ,  $\mu < 0$ ) resonator and filter element. We report a *new caution* of using metamaterial resonator as a filter between DUT and instrument as an attempt to reduce the noise floor. Exciting design choices with  $\epsilon < 0$  or  $\mu < 0$ , however, impedance is not what we are used to. This discussion is imperative for emerging negative index resonator oscillator circuit at microwave and millimeter wave frequency.

**Keywords**—Cross-spectrum, negative index, Oscillator, PN

## I. INTRODUCTION

Phase noise is often the nemesis that limits the performance of a receiving system. Prediction and estimation of oscillator phase noise is highly desirable for accurate timing, and other measuring purposes. Following are the primary PN (phase noise) measurement techniques, listed in the order of increasing precision: (i) Direct Spectrum Technique, (ii) Frequency discriminator method—Heterodyne digital discriminator method, (iii) Phase detector techniques—Reference source/PLL method, (iv) Residual Method, and (v) 2-channel cross-correlation technique. The Direct Spectrum Method, PLL method, delay line discriminator method, and cross-correlation method are frequently used to measure the oscillator phase noise. The first one is the simplest and has the biggest limitation. The last one requires the most complex measurement system but is the most versatile, can measure PN performance better than that of its reference oscillator [1]-[19].

The oscillator noise is normally described in terms of the power spectrum density  $S(f)$  of the amplitude and phase noise, symbolically represented as  $S_a(f)$  and  $S_\phi(f)$  respectively, as a function of the Fourier frequency  $f$ . The first definition of phase noise  $\mathcal{L}(f)$  was given as

$$\mathcal{L}(f) = (\text{SSB power in 1Hz bandwidth})/(\text{carrier power}) \quad (1)$$

The problem with this definition is that it does not differentiate AM noise from PM noise, which leads to ambiguous results. The cross spectrum method is a standard practice in the measurement of oscillator phase noise. It is widely used by manufacturers and customers/users of oscillators, and by academic/public labs as well, including primary labs. In short, the instrument has two separate channels – each consisting of a reference oscillator and a phase detector – which measure simultaneously the oscillator under test (DUT). Assuming that the two channels are statistically independent, the average cross spectrum converges to the DUT

noise spectrum, rejecting the single-channel noise (reference oscillators and a phase detector). The method is inherently prone to experimental errors due to any phenomenon affecting both the channels (correlated). For example, the DUT AM noise yields errors if the phase detector is sensitive to power [1]-[4]. Until recently, this fact was only interpreted as a limitation of the instrument sensitivity, i.e., the lowest PM noise that one can measure. Otherwise stated, most people believe that measurements always result in the over-estimation of the DUT noise because positive instrument noise adds up. This is untrue and correlated noise or stray signals can result in negative-error terms. When this happens, the instrument underestimates the DUT noise, which is undesirable. The phase noise plots of 5 MHz Quartz oscillator shown in Figure (1) clearly identify the artifacts (Courtesy: Nelson et al, NIST).

Theory and simulations suggest that similar physical mechanisms may produce totally wrong spectra, with no identified artifacts. The problems reported went unnoticed for a long time. This is probably related to the small averaging capability of earlier FFT analyzers. The full awareness of this erroneous noise estimation was reported in [4]-[5]. Nelson et al. proposed simulations and a collection of ‘ill-looking’ spectra, pointing out the presence of a problem and experimental conditions for artifacts.

## II. CROSS-SPECTRUM PHASE NOISE MESAUREMENT

The cross-spectrum method provides high sensitivity by correlation and averaging on two equal channels that measures the identical input and rejects the pervasive background noise. Most of the phase noise measurement equipments use default estimated value of background noise, which is twofold higher, because random noise would equally split between real and imaginary part of the cross PSD (power spectral density function).

Figure (2) shows the typical block diagram of the 2-channel cross-correlation/cross-spectrum PN (phase noise) measurement technique. Cross-spectral analysis is a mathematical tool for extracting the power spectral density of a correlated signal from two time series in the presence of uncorrelated interfering signals.

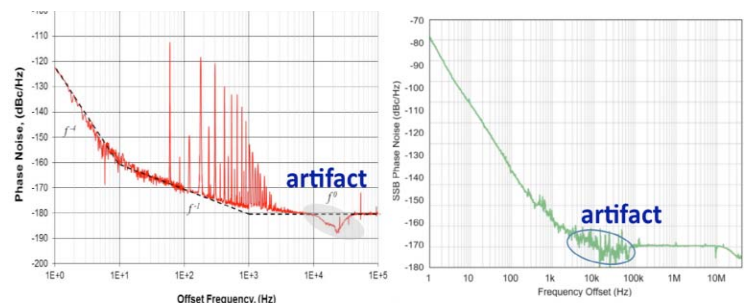


Fig. 1: Phase noise measurement of 5MHz Quartz oscillator: spectra show clearly identified artifacts (Courtesy: NIST)

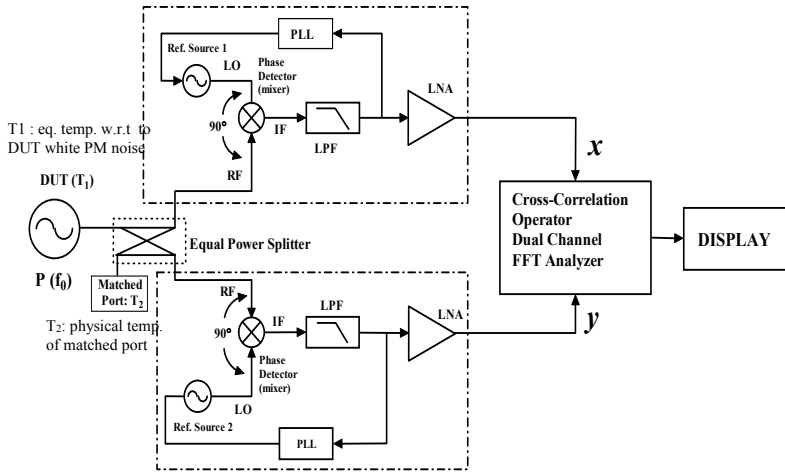


Fig. 2: A typical diagram of 2-channel cross-correlation technique [6]

The oscillator under test is measured simultaneously by two separate phase-to-voltage transducers (in the dashed boxes), and by a dual-channel FFT analyzer. The O/P of each channel as shown in Figure (2) is

$$x(t) = a(t) + c(t) \leftrightarrow X(f) = A(f) + C(f) \quad (2)$$

$$y(t) = b(t) + c(t) \leftrightarrow Y(f) = B(f) + C(f) \quad (3)$$

where  $a(t)$ ,  $b(t)$  and  $c(t)$  are random signals;  $a(t)$  and  $b(t)$  are the noise of the transducers, and  $c(t)$  is the DUT noise; the upper case is used for the Fourier transform, and the ' $\leftrightarrow$ ' stands for the transform / inverse-transform pair.

All signals are sampled at a suitable rate, and each acquisition takes the measurement time  $T$ . The PSD (Power Spectral Density) is a complex concept of mathematical probability, defined as the Fourier transform of the covariance function. The cross PSD is

$$S_{yx}^1(f) = \frac{2}{T} Y(f) X^*(f) \quad (4)$$

where the superscript '1' means single-sided (no negative frequencies) and will be omitted hereinafter; the symbol '\*' means complex conjugate, and the factor '2' is necessary for power consistency, after removing the negative frequencies.

Equation (4) implies the mathematical expectation, which in experiments is replaced with the average over a suitable number ' $m$ ' of samples, denoted with  $\langle S_{yx} \rangle_m$ .

The average measurement takes a time  $mT$ , plus computing time. Using (2)-(3), and omitting ' $f$ ' we get

$$\langle S_{yx} \rangle_m = \frac{1}{mT} \sum_{i=1}^m (B_i A_i^* + B_i C_i^* + C_i A_i^* + C_i C_i^*) \quad (5)$$

Notice that  $B_i A_i^*$ ,  $B_i C_i^*$ , and  $C_i A_i^*$  are in general complex, while  $C_i C_i^*$  is always real.

The random signals  $a(t)$ ,  $b(t)$  and  $c(t)$  are statistically independent because they originate from separate circuits. For the same reason, their Fourier transforms are statistically independent.

As a consequence, the background noise ( $B_i A_i^*$ ,  $B_i C_i^*$ , and  $C_i A_i^*$  terms) are rejected proportionally to  $\frac{1}{\sqrt{m}}$ , and for large  $m$  the average  $\langle S_{yx} \rangle_m$  converges to the DUT noise  $S_{cc}$ .

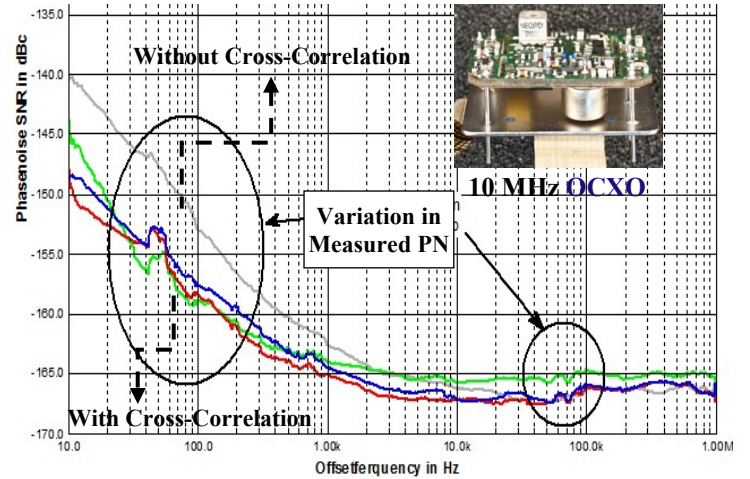


Fig. 3: Measured phase noise plots of 10 MHz OCXO circuit with/without cross-correlation (1000 correlation)

From (5), the DUT noise through each channel is coherent and is therefore not affected by the cross-correlation, whereas, the internal noises generated by each channel are incoherent and diminish through the cross-correlation operation at the rate of  $\sqrt{M}$  ( $M$  = number of correlations), given by

$$[Noise]_{meas} = [Noise]_{DUT} + \frac{[Noise]_{channel1} + [Noise]_{channel2}}{\sqrt{M}} \quad (6)$$

where  $[Noise]_{meas}$  is the total measured noise at the display;  $[Noise]_{DUT}$  the DUT noise;  $[Noise]_{channel1}$  and  $[Noise]_{channel2}$  are the internal noise from channels 1 and 2, respectively; and ' $M$ ' is the number of correlations.

From (6), the 2-channel cross-correlation technique offers superior noise measurement capability but the measurement speed suffers when increasing the number of correlations.

Figure (3) shows the measured 10 MHz crystal oscillator, cross-correlation offers 10-20 dB improvement in PN performance.

From (5)-(6), it is interesting to note that equipments would read default estimated value of background noise, which is twofold higher, because random noise equally distributed between real  $[Re\{\langle S_{yx} \rangle_m\}]$  and Imaginary  $[Im\{\langle S_{yx} \rangle_m\}]$  part. Therefore, for the similar rejection of background noise, it would require 4-times larger value of ' $m$ ' and also measurement time increases by 4 times

### III. VALIDITY OF CROSS-SPECTRUM PN MESAUREMENT

Cross-spectral analysis is a mathematical tool for extracting the power spectral density of a correlated signal from two time series in the presence of uncorrelated interfering signals. A major crux of the system described is the inherent impossibility to differentiate the DUT (device under test) noise from any other correlated effect.

It is self-evident that vibrations or EMI (electromagnetic interference) hitting simultaneously on the two channels as depicted in Figure (2) cannot be rejected. However, this experience is often useful to identify these perturbations as artifacts. Other effects are more subtle, and difficult to identify. The cross-spectrum of two signals  $x(t)$  and  $y(t)$  is defined as the Fourier transform of the cross-covariance function of  $x$  and  $y$ . Introducing a perturbing signal  $d(t)$  impacting the two channels, (2)-(3) may be rewritten as

$$x = a + c + \zeta_x d \leftrightarrow X = A + C + \zeta_x D \quad (7)$$

$$y = b + c + \zeta_y d \leftrightarrow Y = B + C + \zeta_y D \quad (8)$$

where  $\zeta_x$  and  $\zeta_y$  are the coefficients which describe the impact of  $d$  on the phase-to-voltage converters.

Notice that  $\zeta_x$  and  $\zeta_y$ , and also the product  $\zeta = \zeta_x \zeta_y$ , can be either positive or negative. This is the case, for example, of amplitude noise, spurs, and harmonics. For the purpose of this paper, rigorous measurement was conducted in a Faraday cage for the theoretical validation and assumption ( $d$  is statistically independent of  $a$ ,  $b$  and  $c$ ). This approximation has the virtue of giving physical insight on the experimental errors with very simple formalism. Having said that, after averaging on a large  $m$ , the cross PSD converges to

$$S_{yx} = S_{cc} + \zeta S_{dd} \quad (9)$$

The case of  $\zeta > 0$  comes with no surprise, as the experimentalist is familiar to instruments which contribute their own background noise. In the early time, the struggle for better instruments was driven by the idea that a mixer can be operated in a "sweet point" close to the quadrature, where the sensitivity to AM noise nulls. Oppositely,  $\zeta < 0$  means that the instrument systematically under-estimates the DUT noise, as a result of the perturbing signal  $d$ . In some extreme cases  $S_{yx}$  can collapse to zero, or even be negative, which is impossible for the DUT noise. This will be unnoticed in virtually all practical cases, where the displayed quantity is  $[\mathcal{L}(f)]_{\text{dB}} = 10 \cdot \log_{10}(1/2 \cdot |S_{yx}(f)|^2)$ . Multiple perturbing signals  $d_1, d_2, d_3, \dots, d_n$  may show up as bumps or dips. Even worse, if  $C(f)$  and  $D(f)$  have the same shape or slope versus frequency, entire octaves or decades of spectrum can be hideously under-reported, and yet looking like perfectly smooth regions in the polynomial law which describes  $\mathcal{L}(f)$ . Therefore, the detection of the desired signal using cross-spectral techniques collapses partially or entirely in presence of the second uncorrelated interfering signal. The phase noise floor is not limited by the room temperature to a certain extent thermal homogeneity and crosstalk dictates the phase noise floor; unexpectedly, cross-correlation measurement leads to wrong of phase noise floor. Furthermore, error in noise floor measurement can go higher if the bias error  $\left( \frac{k \times T_{\text{Equipment}}}{P(f_0)} \right)$  inborn in thermal energy of the power splitter at the input of the equipment (Fig.2) is not taken into consideration, where  $k=1.38064852 \times 10^{-23} \text{ m}^2 \text{ kg s}^{-2} \text{ K}^{-1}$ .

The existence of unwanted correlated signals due to the thermal energy in the input power splitter would produce correlated thermal noise equal in magnitude but 180 degree out of phase, can give erroneous measurement of DUT noise in dual channels cross-spectrum measurement. The endeavor for overcoming these error by incorporating passive devices (isolator, circulator, filter, resistive splitter and coupler) between DUT (oscillator) and mixer of 2-channel cross spectrum measurement in shown Figure (2) can lead to additional systematic errors because of the impedance mismatch. Fascinatingly, averaging methods used in cross-spectrum PN measurement suppressed the errors even though reflection coefficient is not zero, it introduces coupling between channel at the input of DUT because of mismatch in impedance and phase condition [8].

For homogeneous electrical resonator possessing positive index 'n' ( $n = \sqrt{\epsilon\mu}$ ;  $\epsilon > 0$ ,  $\mu > 0$ ), noise parameter is typically represented using current and voltage sources, whose average values are obtained from the fluctuation dissipation theorem based on normalized impedance [9]. But in non-homogeneous negative index ( $n = -\sqrt{\epsilon\mu}$ ;  $\epsilon < 0$ ,  $\mu < 0$ ) resonator structure, these noise sources degenerates into magneto-inductive noise, lead to the propagation in the form of forward and backward noise waves [10]. Any material supporting single propagating mode at a known frequency, usually exhibits well-defined index ( $n$ ), despite the material is homogeneous/continuous or not. But it is not easy to assign normalized impedance ( $z$ ) to a non-homogeneous material [11].

It is self-evident that multi-mode random spectral signals linked with negative index ( $\epsilon < 0$ ,  $\mu < 0$ ) resonator (Metamaterial Resonator) dynamics hitting simultaneously on the two channels cannot be rejected because of uncertainty associated with wave impedances (forward  $z^+$  and backward  $z^-$ ). Therefore, rigorous measurement was conducted in a Faraday cage for the theoretical validation for giving physical insight on the experimental errors on negative index resonator based voltage controlled oscillator circuit.

#### IV. EXPERIMENTAL VALIDATION: DETECTION AND MITIGATION

##### A. Ex: 2.4 GHz Low Noise SAW Resonator Oscillator

The conventional phenomenological understanding is questionable, which assumes that resonator-operating regime beyond the threshold of nonlinearity, necessarily degrades phase noise. The recent research reported in [12], operating in nonlinear region where the signal level can be increased to large values without the conventionally expected performance phase noise degradation; the improvement in phase noise performance is experimentally verified. It is therefore possible to overcome fundamental limitations of oscillator performance due to thermodynamic noise. As is known for nonlinear resonators, when the driving force is sufficiently large, the system of resonator networks can bifurcate into three possible solutions at a given drive frequency; two of these are stable, and one is unstable [13]. We report results for the oscillator phase noise, focusing in particular, on special operating points of the oscillator where the detrimental effects of the resonator noise are reduced by incorporating dynamically tuned conduction angle feedback circuitry.

Figure (4) shows the typical schematic and layout of ultra low phase noise 2.4 GHz SAW oscillator circuit, where SAW resonator is driven into nonlinear regime window. The improvement in phase noise is achieved by using the feedback phase to tune the oscillator to operating points where the sensitivity to particular noise sources are reduced and choosing a feedback level and phase so that the resonator is driven where the amplitude-frequency and phase-frequency curves of the driven resonator become non-monotonic. PN plots shown in

Figure (5) is the best performance (-150 dBc/Hz @ 10 kHz offset) reported to date for this class technology. The cross-correlation PN measurement technique was applied to isolate any form of injection locking or inadvertent non-linearity, but inherent flaw of phase inversion gave erroneous result.



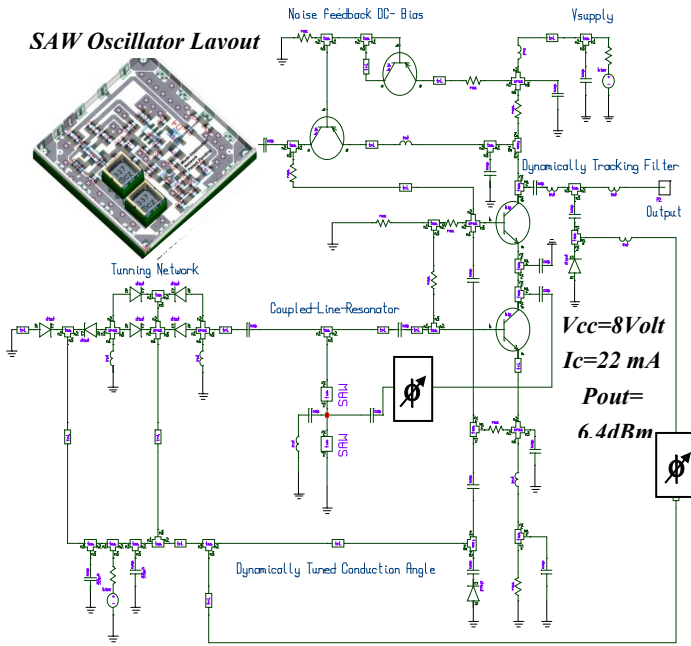


Fig. 4: A typical schematic and layout of 2.4 GHz SAW VCO

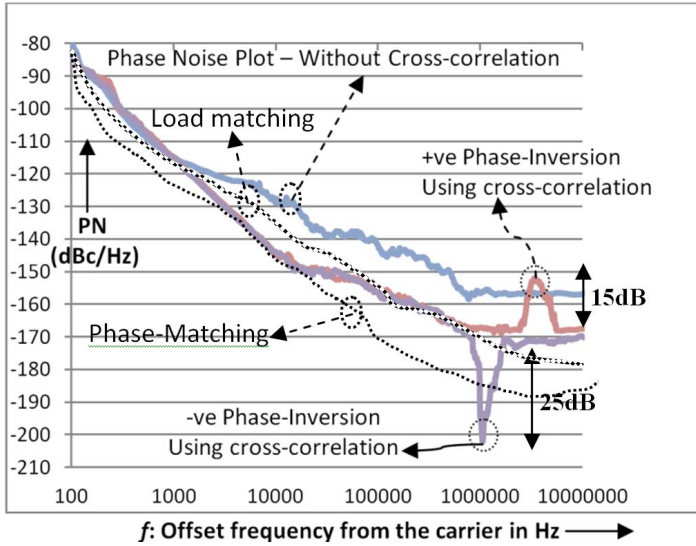


Fig. 5: Measured phase noise plots of 2.4GHz SAW oscillator circuit

The cross-correlation PN measurement technique was applied to isolate any form of injection locking or inadvertent non-linearity, but inherent flaw of phase inversion gave erroneous result. Figure (5) shows the misleading plot for 2.4 GHz SAW oscillator, an optimistic value of  $-202\text{dBc/Hz}$  at 1.2 MHz off the carrier and 15 dB inferior at 6 MHz offset depending upon +ve/-ve phase inversion respectively. The phase in the input path is changed in small steps. We have witnessed the variation in PN measurement due to:

- AM Noise
- Impedance/reflection (Load/phase mismatch)
- Harmonic distortion
- Cable length, cable type (undetected) damages
- Power splitters, Metamaterial Filter/Resonator

These variations can be minimized by incorporating phase-tuned filter and impedance matching at output so that impact of +ve/-ve phase inversion can be reduced significantly.

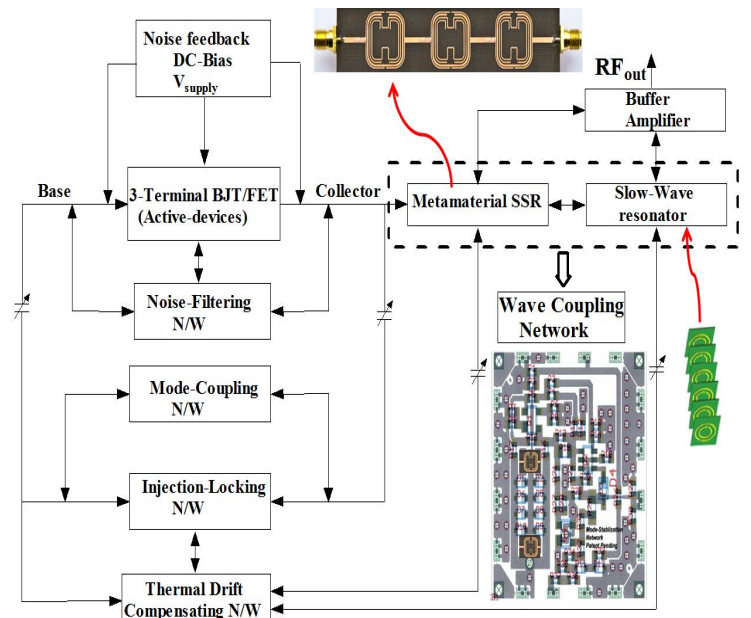


Fig. 6: A typical schematic and layout of negative ( $\epsilon < 0, \mu < 0$ ) index resonator (Metamaterial Resonator) oscillator

### B. Ex: 10.24 GHz Low Noise Negative Index Resonator VCO

Figure (6) shows the typical schematic of X-band oscillator using printed resonator network. As shown in Figure (6), the resonator is realized using negative index material as an energy storing element for realization of high performance signal source at X-band. Based on experimental exercise carried out on 10.239 GHz oscillator, we found that there is a *new caution* of using metamaterial resonator between DUT and PN measurement instrument.

Figure (7) shows the measured phase noise plots of oscillator circuit shown in Figure (6). As shown in Figure (7), various traces (Trace 1, Trace 2, Trace 3, and Trace 4) depict the phase noise plots under following conditions: Trace 1:  $\epsilon > 0, \mu > 0$ ; Trace 2:  $\epsilon > 0, \mu < 0$ ; Trace 3:  $\epsilon < 0, \mu > 0$ ; and Trace 4:  $\epsilon < 0, \mu < 0$ .

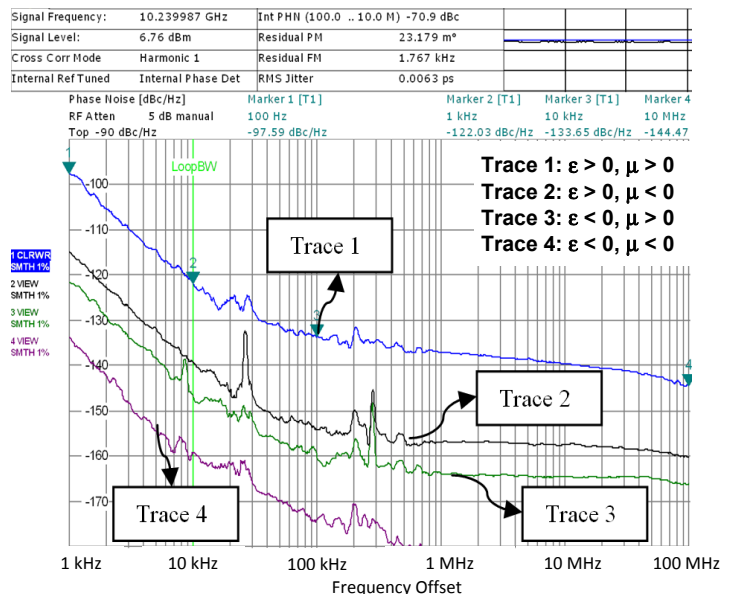


Fig. 7: Measured phase noise plots of 10.239 GHz oscillator (Fig. 6)

The multi-mode spectrum associated with negative index medium can mislead the data if due care is not taken during measurement. Exciting design choices with  $\epsilon < 0$  or  $\mu < 0$ , however, impedance is not what we are used to. The negative index material ( $\epsilon < 0$ ,  $\mu < 0$ ) based resonator exhibits different values of wave-impedances for forward and backward wave propagating direction [15].

It is to note that negative index material ( $\epsilon < 0$ ,  $\mu < 0$ ) structure does not exhibit distinct impedance ( $z$ ) values because ratio of electric/magnetic field will vary periodically throughout the structure. The real challenge is the existence of nonlinear impedance and also lack of a unique definition for  $z^\pm$  indicates that the significant variation in the phase noise measurements.

It is to note that multiple physically separated tuning diodes connected to negative index material ( $\epsilon < 0$ ,  $\mu < 0$ ) resonator structure exhibits reduction in noise as compared to equivalent larger single tuning diode. The possible explanation could be evanescent mode EM coupling between physically separated diodes lower the noise. However, for a certain case, 2-channel cross-spectrum PN measurement can give optimistic result for multiple tuning diodes physically separated, while keeping the similar value of capacitive ration for a given tuning range.

C. Ex: 100 MHz Crystal Resonator Oscillator Circuit

Figures (8) and (9) show the typical schematic of 100 MHz OCXO and prototype unit fabricated for the validations.

Figures (10), (11), and (12) depict the measured phase noise plots at various conditions for the lowering the phase noise. As shown in Figure (13), the efforts to get low floor can invite troubles that go with the optimization of the floor [14].

As shown in Figure (14),  $I_R$  is transferred and amplified at output. For  $f > v/2Q$ , the thermal noise associated with  $R_s$  is not coupled to buffer, magic bias can reduce the RBB' noise at output.

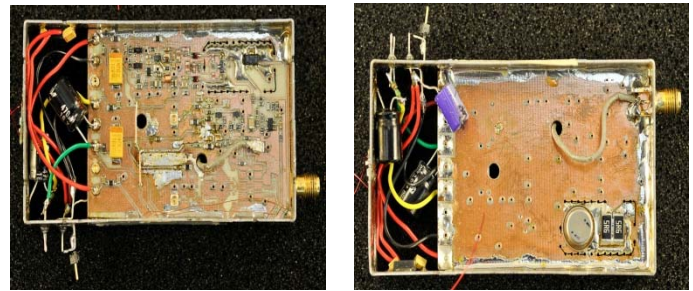


Fig.9 Prototype of a 100 MHz OCXO as per schematic shown in Fig. 8

Signal Frequency:	100.000002 MHz	Int PHN (10.0 .. 10.0 M)	-98.5 dBc
Signal Level:	12.64 dBm	Residual PM	958.696 $\mu^\circ$
Cross Corr Mode	Harmonic 1	Residual FM	22.095 Hz
Internal Ref Tuned	Internal Phase Det	RMS Jitter	0.0266 ps

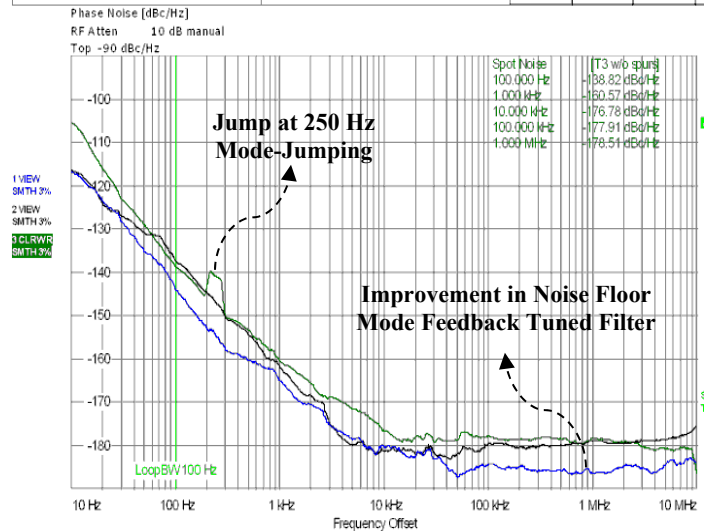


Fig. 10: Measured phase noise plots of 100 MHz OCXO shown in Fig. 9

Signal Frequency:	100.000001 MHz	Int PHN (10.0 .. 10.0 M)	-96.2 dBc
Signal Level:	13.38 dBm	Residual PM	1.256 $m^\circ$
Cross Corr Mode	Harmonic 1	Residual FM	19.998 Hz
Internal Ref Tuned	Internal Phase Det	RMS Jitter	0.0349 ps

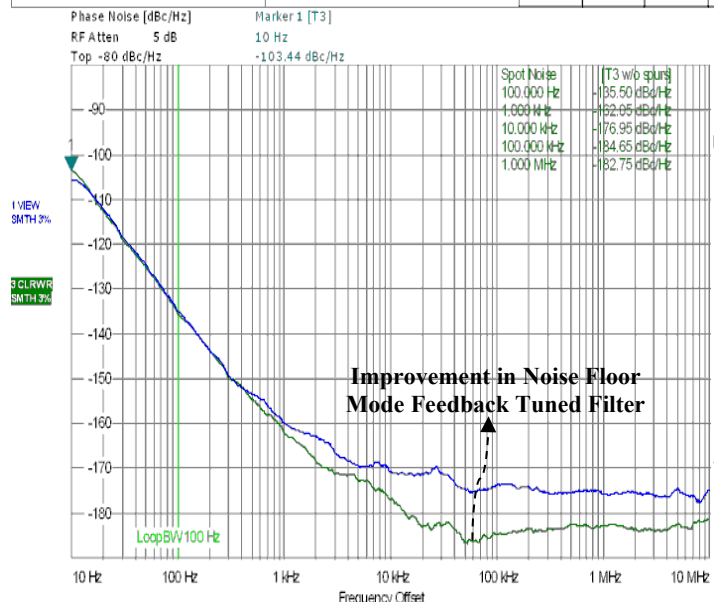
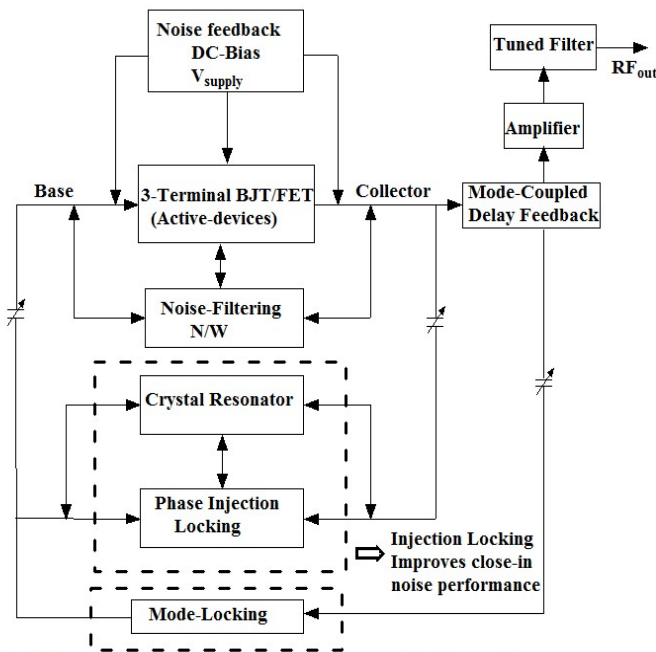


Fig. 11: Measured phase noise plots of 100 MHz OCXO shown in Fig. 9



Mode-Locking and Tuned Filter at O/P Improves far offset noise performance

Fig. 8: A typical schematic and layout of 100 MHz OCXO

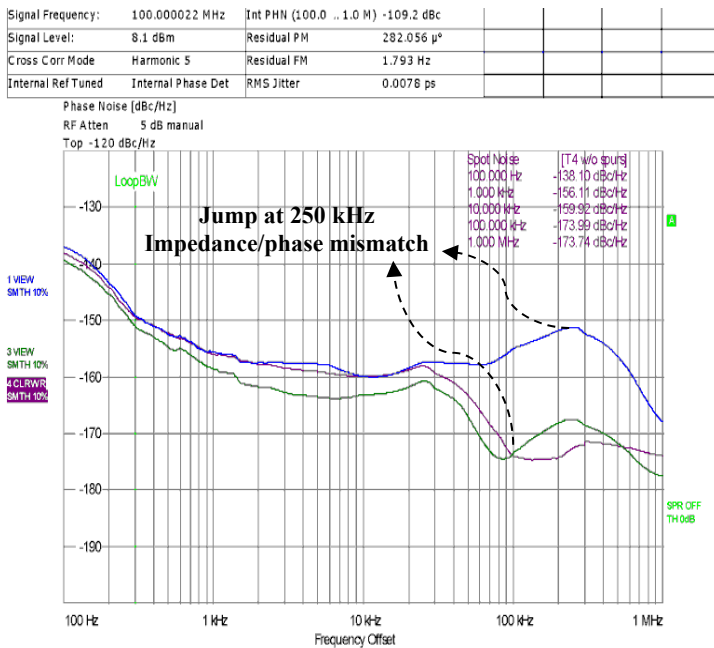


Fig. 12: Measured phase noise plots of 100 MHz OCO shown in Fig. 9

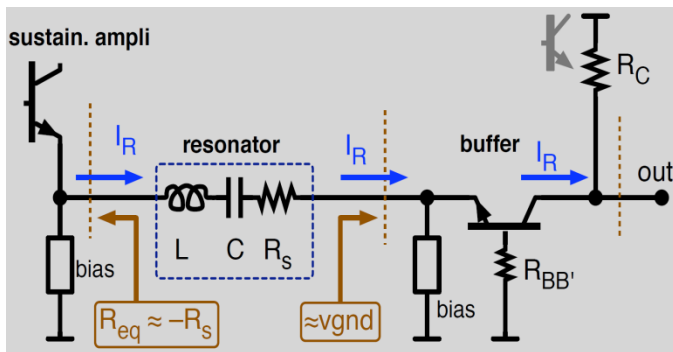


Fig. 13: shows the scheme to get low noise floor

The steps towards minimizing error in PN measurement carried out include, incorporating impedance/phase-matching, absorptive harmonic filters, AM rejection to prevent anti-correlation, optimizing level of mixers as a phase detector (low level, medium level, and high level), and power splitter (reactive and resistive) to minimize anti-correlation. Careful study and measurement was performed on both active (transistors) and passive devices (resistors, inductors, capacitors), it is found that multiple devices separated physically by optimum distance can lower the intrinsic noise; this is due to higher order mode convergence (exhibit energy harvesting) via EM coupling. It is recommended to use multiple physically separated small size devices (tuning diodes, resistors) as a substitute of single large device [15]-[16].

## V. CONCLUSION

The concern of PN measurement in presence of negative index can give erroneous results. In addition to this, due care must be taken to compensate the error due to thermal energy associated with components (power splitter) used in dual-channel cross-spectrum measurement techniques that uses dual-PD. Exciting design choices with  $\epsilon < 0$  or  $\mu < 0$  are possible, however, dynamic impedance associated with negative index

resonator and filter is not what we are used to. We have witnessed the variation in PN measurement due to:

- AM Noise
- Impedance/reflection (Load/phase mismatch)
- Harmonic distortion
- Cable length, cable type (undetected) damages
- Power splitters

Based on experimental exercise carried out in this paper, we found that there is a *new warning* of using negative index material (Metamaterial) as a filter between DUT and PN measurement instrument.

## REFERENCES

- [1] S. Sancho et al, "Analysis of near-carrier phase-noise spectrum in free-running oscillators in the presence of White and colored noise sources". IEEE Trans. MTT, Vol. 58, No. 3, pp. 587-601, March 2010
- [2] E. Rubiola, F. Vernotte, "The cross-spectrum experimental method," February 2010, arXiv:1003.0113 [physics.ins-det]
- [3] E. Rubiola, R. Boudot, "The effect of AM noise on correlation phase noise measurements." IEEE Transact. Ultrason., Ferroelec. Freq. Control 54(5) p. 926-932, May 2007.
- [4] C. W. Nelson, A. Hati, and D. A. Howe, "A collapse of the cross-spectral function in phase noise metrology," Rev. Sci. Instrum. 85, 024705 (2014). See also Proc. IFCS 2014 (Taipei, Taiwan).
- [5] U. L. Rohde, A. K. Poddar, "Phase Noise Measurement Techniques, Associated Uncertainty and Limitations," Proc. 2013 IFCS EFTF Joint Meeting p.438-441, 21-25 July 2013.
- [6] A. K. Poddar, U. L. Rohde, S. K. Koul, E. Rubiola, and M. A. Silaghi, "Cross-Correlation PN Measurements: Pros & Cons", 2015 IEEE IMArc, Hyderabad, Dec 10-12, 2015.
- [7] A. K. Poddar, "A Novel Approach for Designing Integrated Ultra Low Noise Microwave Wideband VCO, Ph.D. Thesis, TU-Berlin, Germany, Dec 2004.
- [8] A. K. Poddar, "Slow Wave Resonator Based Tunable Multi-Band Multi-Mode Injection-Locked Oscillators" Dr.-Ing.-habil Thesis, BTU Cottbus, 2014.
- [9] H.B. Callen, T.A. Welton "Irreversibility and generalized noise" Phys. Rev. Vol. 83, No. 1, pp. 34-40 (1951)
- [10] Smith et al, "Determination of effective permittivity and permeability of Metamaterials from reflection and transmission coefficients," Phys.Rev. B, Vol. 65, No. 19, 195104, 2002
- [11] R. R. A. Syms, O. Sydoruk, and L. Solymar, "Noise in one-dimensional metamaterials supporting magnetoinductive lattice waves", APS, Physical Review B 87, pp. 155155 (1-8), 2013
- [12] Villanueva et al, "Surpassing Fundamental Limits of Oscillators Using Nonlinear Resonators", Phys Rev Lett. 2013 April 26; 110(17): 177208
- [13] R. Lifshitz, M. Cross, "Reviews of Nonlinear Dynamics and Complexity. Schuster", Vol. 1. Wiley-VCH; Weinheim: 2008. p. 1-52.
- [14] U. L. Rohde, Electronic Design 21 p.11-14, Oct 11, 1975.
- [15] A. Poddar, "Slow wave resonator based tunable multi-band multi-mode injection-locked oscillator", Habil Thesis, BTU Cottbus, Germany, 2014
- [16] Ajay K. Poddar, Ulrich L. Rohde, Anisha M. Apte, "How Low Can They Go, Oscillator Phase noise model, Theoretical, Experimental Validation, and Phase Noise Measurements", IEEE Microwave Magazine, Vol. 14, No. 6, pp. 50-72, September/October 2013.
- [17] Ulrich L. Rohde, Ajay K. Poddar, Anisha M. Apte, "Getting Its Measure", IEEE Microwave Magazine, Vol. 14, No. 6, pp. 73-86, September/October 2013.
- [18] Ajay K. Poddar and Ulrich L. Rohde, "Crystal Oscillators", Wiley Encyclopedia and Electronics Engineering", pp.1-38, Oct. 2012.
- [19] Ajay K. Poddar and Ulrich L. Rohde, "Crystal Oscillator Design", Wiley Encyclopedia of EEs Engg, pp. 1-47, Oct. 2012.